THE ORIGIN OF STAR FORMATION GRADIENTS IN RICH GALAXY CLUSTERS

Michael L. Balogh[1] and Julio F. Navarro[2]
Dept of Physics and Astronomy, University of Victoria
P.O. Box 3055, Victoria, B.C. V8W 3P6, Canada
Simon L. Morris
Dominion Astrophysical Observatory
Herzberg Institute of Astrophysics, National Research Council of Canada
5071 W. Saanich Rd., Victoria, B.C. V8X 4M6, Canada

ApJ, resubmitted Mar 31, 2000

ABSTRACT

We examine the origin of clustercentric gradients in the star formation rates and colors of rich cluster galaxies within the context of a simple model where clusters are built through the ongoing accretion of field galaxies. The model assumes that after galaxies enter the cluster their star formation rates decline on a timescale of a few Gyrs, the typical gas consumption timescale of disk galaxies in the field. Such behaviour might be expected if tides and ram pressure strip off the gaseous envelopes that normally fuel star formation in spirals over a Hubble time. Combining these timescales with mass accretion histories derived from N-body simulations of cluster formation in a ΛCDM universe, we reproduce the systematic differences observed in the color distribution of cluster and field galaxies, as well as the strong suppression of star formation in cluster galaxies and its dependence on clustercentric radius. The simulations also indicate that a significant fraction of galaxies beyond the virial radius of the cluster may have been within the main body of the cluster in the past, a result that explains naturally why star formation in the outskirts of clusters (and as far out as two virial radii) is systematically suppressed relative to the field. The agreement with the data beyond the cluster virial radius is also improved if we assume that stripping happens within lower mass systems, before the galaxy is accreted into the main body of the cluster. We conclude that the star formation rates of cluster galaxies depend primarily on the time elapsed since their accretion onto massive virialized systems, and that the cessation of star formation may have taken place gradually over a few Gyrs.

1. INTRODUCTION

Extensive observational work has established that the star formation properties of galaxies in rich clusters differ significantly from those of field galaxies (e.g., **?**; **?**; **?**; **?**). In the field, galaxies form stars at rates several times higher than systems of similar luminosity in the cores of clusters. This is partly a result of the well-known morphology-density relation, since ellipticals and S0 galaxies are more abundant in clusters (**?**; **?**), but there is evidence that even later type galaxies in clusters form stars at lower rates then in the field. For example, Balogh et al (**?**) report that field galaxies of given bulge-to-disk ratio and luminosity have, on average, much larger [OII] equivalent widths than their counterparts in rich clusters, suggesting that the cluster environment somehow curbs the star formation rates of all galaxies, regardless of morphology.

Various physical mechanisms have been proposed to explain this and other systematic differences between the field and cluster galaxy populations. Ram pressure stripping by the intracluster medium, for example, has been suggested as a means of removing the gaseous component of disk galaxies and of dramatically altering their morphology and subsequent star forming history (e.g., **?**; **?**; **?**). Tides, either by the main cluster potential (e.g. **?**; **?**) or by fly-by encounters with other cluster galaxies ("galaxy harassment", **?**), have also been proposed to explain the observations.

Although the above processes are all plausible, the actual changes in star formation rate induced by them remain a matter of debate. For example, some authors have suggested that the cluster environment triggers intense bursts of star formation that rapidly consume the gas of an infalling cluster galaxy (**?**; **?**; **?**), while others have favored a scenario where star formation is truncated in a galaxy almost immediately after it is accreted into the cluster (**?**; **?**; **?**; **?**).

The virtues of these scenarios can in principle be tested observationally, since they are expected to produce a population of galaxies with unusually strong Balmer absorption lines in which star formation has been recently terminated (e.g., **?**; **?**). Recently, Balogh et al. (**?**) have applied this idea to galaxies in the CNOC1 survey of X-ray luminous clusters (**?**). From the paucity of galaxies with strong Hδ absorption in their spectra they conclude that the decline of star formation in these clusters may actually be a fairly gradual process. This is in contradiction to other authors' conclusions, which are derived from datasets with relatively high numbers of Hδ-strong objects (e.g. **?**; **?**); whether this discrepancy is due to selection effects or to real differences in the clusters studied has not yet been fully elucidated.

A natural timescale for a gentler reduction in star for-

[1]Present address: Department of Physics, University of Durham, South Road, Durham UK DH1 3LE
email: M.L.Balogh@durham.ac.uk

[2]CIAR Scholar and Alfred P. Sloan Foundation Fellow

mation rate may be gleaned from the long–known observation that, given their present disk gas content, normal field spirals currently form stars at rates that cannot be sustained over a Hubble time. At face value, it appears that most spirals would use up their disk gas supply in a few Gyrs (e.g., **?**), though this timescale may be considerably extended for some choices of the IMF and if the effects of non-instantaneous mass recycling is taken into account (**?**). Star formation lifetimes can be significantly longer if galaxies continuously accrete fresh star formation fuel from their surroundings (e.g., **?**). If, as proposed by Larson, Tinsley & Caldwell (**?**), this extended reservoir is stripped off a galaxy when it first enters the cluster, its star formation rate may decay significantly within a few Gyr, leading to large differences in the cluster and field populations. In clusters that are built hierarchically (as in the "bottom-up" scenario favored by cold dark matter cosmogonies) this mechanism would also establish a radial gradient in the star formation properties of cluster galaxies, reflecting the relation between the clustercentric radius of a galaxy and the time of its accretion into the cluster. This is an important ingredient in the success of semi-analytic models, which have been shown to match global cluster properties such as the morphological composition and the blue galaxy fraction (**?**; **?**).

We explore here a simple model based on this interpretation where the mass accretion history of a cluster obtained from numerical simulations of a universe dominated by cold dark matter is coupled with a simple star formation prescription for galaxies following accretion. Once calibrated to reproduce the properties of local field galaxies, the model has no free parameters and its results can be compared directly with observations. We shall focus our analysis on a quantitative discussion of the clustercentric radial gradients in star formation properties and galaxy colors expected in this model.

In §2 we describe the observational dataset we use, selected from the CNOC1 survey. The numerical simulations used to derive mass accretion histories of different clusters are described in §3. Our model prescriptions are presented in §4 and our results in §5. We discuss the implications of our results in §6, and list our conclusions in §7.

2. OBSERVATIONAL DATASET

We use in this paper the CNOC1 cluster redshift survey dataset (**?**), which consists of CFHT spectra for ~ 2000 galaxies in 15 X–ray luminous clusters at $0.19 < z < 0.55$. The observational selection effects of this survey are well understood and are discussed in detail in Yee, Ellingson & Carlberg (**?**) and Balogh et al. (**?**). For the present analysis, we weigh the raw data by three factors: one to account for the primary selection effect due to source magnitude, and two secondary corrections which depend on the galaxy color and position on the CCD. One of the main advantages of this survey, especially for the purposes of the present study, is that the dataset includes spectra of foreground and background field galaxies projected onto each cluster. Since both field and cluster galaxies are selected using the same criteria, *relative* differences between the two samples are rather insensitive to uncertainties in the procedure used to correct for selection effects.

Since our analysis concentrates on radial gradients within clusters, we only consider those clusters with well defined centers in position and velocity space and thus exclude from the sample the bimodal clusters MS0906+11 and MS1358+62 (**?**). We also restrict the redshift range of the galaxy sample to $0.19 < z < 0.45$, in order to facilitate comparisons with simulations analyzed at a single epoch and to minimize effects due to global changes in the galaxy population as a function of redshift. This effectively removes two more clusters from the CNOC1 sample, MS0016+16 and MS0451-03. The final sample has twelve clusters in total, which are scaled and co-added together to construct a "fiducial cluster" sample where effects due to substructure and asphericity of individual clusters are minimized (**?**). The full procedure is described in detail in Balogh et al (**?**; **?**).

In brief, we use the mass models of Carlberg, Yee & Ellingson (**?**) to divide the sample into a cluster and field sample; galaxies are deemed to be cluster members if they are within 3σ of the (radially dependent) cluster velocity dispersion, and field members if they are beyond 6σ. Cluster galaxy positions are all measured relative to the brightest cluster galaxy (BCG), and normalized to R_{200}, the radius at which the mean inner density is 200 times the critical density. The BCGs themselves are omitted from the final sample, as they are likely to have a unique formation history which may differ from the general cluster population; we briefly compare their properties with those of the full sample in §5.1. Finally, we impose an absolute magnitude limit on the sample, considering only galaxies brighter than $M_r = -18.5 + 5\log h$ at $z = 0$ (Gunn-r, $q_0 = 0.1$); when appropriately weighted, this sample is statistically complete. Because each individual cluster is at a different redshift a small evolutionary correction is applied to this cutoff assuming that luminosity increases in direct proportion to $(1 + z)$ (e.g., **?**). At $z \sim 0.3$, the luminosity cutoff we adopt is therefore $M_r = -18.8 + 5\log h$. This correction has little effect on our results because of the narrow redshift range under consideration. For the sample considered here, the luminosity function of the cluster population is similar to that of the field galaxy population.

Individual star formation rates (SFRs) for galaxies in the sample are computed from the rest frame equivalent width of the [OII]λ3727 emission line and the rest frame B–band luminosity relative to solar ($L_B/L_{B,\odot}$) using the relation,

$$\dot{M}_* = 3.4 \times 10^{-12} \left(\frac{L_B}{L_{B,\odot}}\right) W_\circ(\mathrm{OII})\, \mathrm{E(H}\alpha)\, \mathrm{M}_\odot\ \mathrm{yr}^{-1}. \quad (1)$$

Here E(Hα) is the extinction at Hα which, following Kennicutt (**?**), we take to be one magnitude. The coefficient in Equation 1 has been chosen so that, on average, the SFRs of field galaxies are consistent with their colors and luminosities, based on models of their star formation history that are discussed in detail in §5.2. This coefficient is consistent with that empirically determined by Barbaro & Poggianti (**?**), and about 30% larger than that measured by Kennicutt (**?**) — well within the uncertainty of its determination (see Kennicutt **?**). Because we are concerned with relative differences, neither this normalization nor the extinction correction has a significant effect on our conclusions, unless these quantities vary dramatically from the cluster to the field.

Uncertainties in the equivalent widths have been assessed assuming Poisson statistics, and have been internally calibrated to account for additional systematic errors, as described in Balogh et al. (**?**). We exclude from the sample all galaxies with very large $W_\circ$(OII) uncertainties, $\Delta\, W_\circ$(OII)$>$ 15Å ($\sim$ 6% of the sample), and all galaxies for which [OII]λ3727 lies outside the observed spectral range. The final sample with measured SFRs consists of 556 cluster galaxies and 339 field galaxies.

The $W_\circ$(OII) measurements from which we derive SFRs are computed by adding up the observed flux (accounting for partial pixels) above the continuum level in the wavelength range $3713 < \lambda/\text{Å} < 3741$. The continuum level is estimated by fitting a straight line to the flux in the ranges $3653 < \lambda/\text{Å} < 3713$ and $3741 < \lambda/\text{Å} < 3801$. For weak or absent [OII] features, the $W_\circ$(OII) index will be sensitive to features in the continuum in these two regions. A crude estimate of uncertainties introduced in the $W_\circ$(OII) measurements by these features may be obtained by using eq. 1 to compute SFRs of galaxies expected to have little or no ongoing star formation; these are red cluster galaxies with large 4000Å breaks ($(g-r)_\circ > 0.35$, $D_{4000} > 1.8$) found within $0 < R/R_{200} < 0.3$. The 3σ–clipped mean SFR of this population is -0.057 $h^{-2}\, M_\odot\, \mathrm{yr}^{-1}$, and the standard deviation is $0.156\, h^{-2}\, M_\odot\, \mathrm{yr}^{-1}$. This small systematic offset and uncertainty are taken into account in our modeling, as described in §4.2.

3. NUMERICAL SIMULATIONS

Cluster mass accretion rates are computed directly from N–body simulations of the formation of six massive clusters ($0.7 < M/(10^{15} M_\odot) < 2.3$) in a COBE-normalized, $\Lambda = 0.7$, $\Omega_0 = 0.3$ cosmology. The simulations are similar to those described in detail by Eke, Navarro, & Frenk (**?**). We assume that "light traces mass" in the clusters and identify statistically each dark matter particle with a "galaxy". The virial radius, $R_{\rm vir}$, of a cluster is computed using the overdensity prescription described in Eke, Cole & Frenk (**?**), which differs slightly from R_{200}. At $z = 0.3$, the mean redshift of our cluster sample, $R_{\rm vir} \approx 1.2 R_{200} \approx 1.4$-2.4 Mpc. Each cluster has about $9,000$ particles within $2\, R_{\rm vir}$ at $z = 0.3$. The observations and model parameters are all presented in terms of the simulation cosmology; we use $H_0 = 70$ km s^{-1} Mpc^{-1}, which gives a present age of the universe of 13.5 Gyr. At $z = 0.3$ the universe is ~ 11 Gyr old.

4. THE MODEL

As discussed in §1, our modeling assumes that cluster galaxies differ from their field counterparts in their star forming properties because they are stripped of their surrounding gas reservoirs as they are accreted into the cluster. Star formation in cluster galaxies thus declines after accretion as more and more of the galaxy's remaining gas content gets turned into stars.

The model involves the following steps:

(i) All particles within $2\, R_{200}$ from the center of each simulated cluster at $z \sim 0.3$ are selected.

(ii) Each particle is traced back in time to find out when it was first accreted into the cluster. Two definitions of "accretion time", $t_{\rm acc}$, are used. The first ($t_{\rm acc} = t_{\rm cluster}$) is defined to be the time when the particle ("galaxy") first finds itself within $R_{\rm vir}$ from the center of the current most massive progenitor of the cluster, and the second ($t_{\rm acc} = t_{\rm group}$) is the time when a galaxy is first accreted into any large clump, not necessarily the most massive one. Details of this procedure are given in §4.1.

(iii) A SFR is chosen for each galaxy at $t = t_{\rm acc}$. For simplicity, these are taken at random (using appropriate weights as discussed in §2) from the distribution of SFRs computed for $z \sim 0.3$ field galaxies in our sample. This assumes implicitly that field SFRs do not evolve with time, arguably the simplest possible model. We explore in §5.2 the consequences of relaxing this assumption.

(iv) We use a simple gas consumption model to estimate SFRs following accretion and to compute the SFR of each cluster galaxy at $z \sim 0.3$. Details are discussed in §4.2.

(v) Each simulated cluster is projected onto three orthogonal planes. Field contamination in the observational sample is accounted for as discussed in §4.3.

This procedure uniquely defines a final ($z = 0.3$) SFR for each galaxy in the simulated clusters; the mean SFR can then be computed as a function of clustercentric distance, and compared with the field galaxy observations. We discuss now the various steps of the model in some detail.

4.1. *Accretion Times*

We have explored two ways of assigning "accretion times", $t_{\rm acc}$, to galaxies in the simulated clusters. One choice defines $t_{\rm acc} = t_{\rm cluster}$ as the time when a particle is first found within the virial radius of the most massive progenitor present at that time. Following Eke, Cole & Frenk (**?**), the virial radius, $R_{\rm vir}$, is defined as the radius where the mean inner density of the cluster is $\bar{\rho}(R_{\rm vir}) = \Delta_c(z)\rho_c(z)$, where $\rho_c(z)$ is the critical density at the redshift z, and $\Delta_c(\Omega(z))$ is the "critical" overdensity for spherical collapse (which takes the familiar value of 178 for $\Omega = 1$ models).

The above definition of $t_{\rm cluster}$ may not be completely appropriate, since in a hierarchically clustering universe particles may be first accreted into another "protocluster" before being accreted into the main progenitor of the final cluster. Therefore, we consider as an alternative definition of $t_{\rm acc}$ the time when a particle first finds itself associated with a clump with circular velocity exceeding $V_c = 500$ km s^{-1}. (This circular velocity corresponds to a virial temperature of ~ 0.8 keV). Particles are associated with clumps via a friends-of-friends algorithm, with an evolving linking length parameter taken to be 10% of the mean inter-particle separation at each time. Accretion times defined this way are labeled $t_{\rm group}$. We shall see in §5.1 that our results are rather insensitive to the particular choice of accretion time definition.

The "resolution" of $t_{\rm acc}$ is limited by the number of times particle positions are output by the simulations. In this case, we have outputs every 1.34 Gyr; we therefore add a uniform random number between 0 and 1.34 Gyr to each particle's $t_{\rm acc}$ to smooth out this resolution. We do not expect our results to be sensitive to this resolution, since we are combining the results of six clusters, which will smooth out the effect of discrete merger events.

4.2. *Star Formation Prescription*

For normal, field spiral galaxies, the SFR per unit area averaged over the disk, $\Sigma_{\rm SFR}$, depends on the disk gas content in a manner well approximated by a Schmidt law (**?**). From Kennicutt (**?**), this relation is given by

$$\Sigma_{\rm SFR} = (2.5 \pm 0.7) \times 10^{-4} \left(\frac{\Sigma_{\rm gas}}{M_\odot {\rm pc}^{-2}} \right)^N M_\odot \, {\rm yr}^{-1} \, {\rm kpc}^{-2}, \quad (2)$$

where $\Sigma_{\rm gas}$ is the average gas surface density, and the exponent $N = 1.4 \pm 0.15$. Converting surface densities to integrated values using the source diameters tabulated by Kennicutt, galaxies that evolve according to this relation and accrete no extra gas would form stars at a steadily decreasing rate given by,

$$\dot{M}_*(t') = \dot{M}_*(0) \left(1 + 0.33 \frac{t'}{t_e} \right)^{-3.5} M_\odot {\rm yr}^{-1}, \quad (3)$$

where $\dot{M}_*(0)$ is the initial SFR and $t_e \approx 1.48 \, (\dot{M}_*(0)/M_\odot \, {\rm yr}^{-1})^{-0.29}$ Gyr is the characteristic gas consumption timescale. As discussed in §4, we adopt $\dot{M}_*(0)$ values taken at random from the measured field SFRs and set $t' = t - t_{\rm acc}$. With these assumptions it is possible to compute SFRs of cluster galaxies at $z \sim 0.3$, the mean redshift of the observational sample. In the above calculation, we have neglected the effects of gas recycling. If we assume instantaneous recycling, where a fraction R of every solar mass of stars formed is returned as gas, the timescale t_e is increased by a factor $1/(1-R)$. Assuming $R = 0.33$ (**?**)[3], we obtain $t_e \approx 2.2 \, (\dot{M}_*(0)/M_\odot \, {\rm yr}^{-1})^{-0.29}$ Gyr. This increase does not have a significant effect on the results we present, so we neglect the effects of recycling throughout this work.

Finally, we correct the values obtained from eq. 3 for the systematic offset and uncertainty in the SFR measurements discussed in §2. This is done by adding a random number, drawn from a Gaussian distribution with a mean of $-0.12 M_\odot$ yr^{-1} and a variance of $0.32 M_\odot$ yr^{-1}, to the model SFR. These parameters were chosen from the SFR distribution of red, central cluster galaxies (with $h = 0.7$), as described in §2.

4.3. *Field Contamination*

Observational cluster datasets are contaminated by field galaxies, projected onto the cluster, that have Hubble-flow redshifts similar to the peculiar velocities induced by the cluster potential. Our model takes this into account following the procedure of Carlberg et al. (**?**). In brief, the velocity differences between cluster and individual galaxies in each dataset are scaled to the velocity dispersion of each cluster and their clustercentric projected radii to R_{200}. These normalized velocities, $V_{\rm norm} = \Delta v/\sigma$, and radii, $R_{\rm proj}/R_{200}$, are then combined into a single dataset. The density of galaxies per unit $V_{\rm norm}$ at $5 < V_{\rm norm} < 25$ is computed in radial bins to account for the radially varying σ. Under the assumption that this density remains constant within each bin, it is used to calculate the expected number of interloper galaxies, i.e., those within 3σ in each radial bin. This provides a direct estimate of the fraction of galaxies deemed cluster members that are actually field galaxies projected onto the cluster in "redshift space". This fraction is typically $\sim 1\%$ in the central cluster regions, but may be as large as $\sim 12\%$ at R_{200}. Our modeling accounts for this effect by including an appropriate number of "field" galaxies (randomly selected from the field sample) in all computations.

5. RESULTS

5.1. *Non-evolving field SFR model*

Figure 1 shows the mean SFR per galaxy as a function of projected distance from the cluster center, normalized to R_{200}. The solid squares correspond to the CNOC1 data for the complete sample of galaxies brighter than $M_r = -19.6$ (at $z = 0.3, h = 0.7$), averaged over radial bins and with 1-σ jackknife error bars. The mean SFR per galaxy increases systematically from the center of the cluster outwards, from almost zero near the center to about $\sim 0.7 \, M_\odot$ yr^{-1} in the outskirts of the cluster. We note that the absolute SFR values quoted here are sensitive to a number of sample selection parameters; in particular to the luminosity cutoff and the uncertain coefficient in eq. 1, so care must be exercised when comparing these results to other work. On the other hand, relative differences between cluster and field populations are robust, since the two samples have similar luminosity functions, and are drawn from the same survey with identical selection criteria.

As shown in Figure 1, the average SFR per galaxy in the field is significantly higher than in clusters. Remarkably, even at radii as far from the center of the cluster as $\sim 2R_{200}$, cluster star formation rates remain depressed by almost a factor of two relative to the field.[4]. We note here that the BCGs, which are omitted from the data sample, have unusually high SFRs; the mean SFR of the 11 BCGs which satisfy our selection criteria[5] is 14 $M_\odot$ yr^{-1}, much greater than the mean field value. Only four of these eleven galaxies have no significant [OII] emission. The low redshift BCGs are discussed in more detail in Davidge & Grinder (**?**); we do not consider these galaxies further in this study.

Figure 1 also shows, with open symbols, the results of the modeling procedure outlined in §4. Open squares and triangles correspond to the two different accretion time definitions discussed in §4.1. Error bars represent the 1-σ variance of the 18 numerical realizations (6 simulated clusters and 3 orthogonal projections per cluster). The agreement between the model and the observations is remarkable, especially considering that the modeling involves no free parameters. The model reproduces the observed SFR gradient and even the observed depression, relative to the field, of SFRs outside R_{200}.

The latter result is somewhat surprising, since in spherical accretion models particles outside R_{200} are infalling

[3]This large factor of R approximates the effects of a non-instantaneous recycling calculation, assuming a Scalo IMF, and is fairly good for slowly evolving disks; for rapidly evolving disks, R can be as high as 0.75.

[4]Because the luminosity functions of the field and cluster population considered in this sample are quite similar, the same result is obtained for the SFR per unit luminosity as for the SFR per galaxy.

[5]No spectrum is available for the BCG in MS 0451.5+0250.

into the cluster for the first time (**?**; **?**) and therefore their SFRs have yet to feel the effects of the cluster environment. The main reason for our result is that a substantial fraction ($54 \pm 20\%$ for the six clusters we studied) of particles between 1 and $2\,R_{200}$ have actually been inside the virial radius of the main progenitor at some earlier time. These are often particles that populated the outskirts of recently accreted clumps and that, although still bound to the system, have been scattered to large apocenter orbits during the merger process.

Interestingly, assuming that the onset of the SFR decline occurs when a galaxy is accreted into *any* clump with circular velocity exceeding 500 km s^{-1} rather than the cluster's main progenitor has only a small effect on this result within R_{200} (witness the good agreement between open triangles and squares in Figure 1). Note that the mean SFR beyond R_{200} is further suppressed under this assumption, resulting in even better agreement with observations. This is because some particles beyond R_{200} are found within fairly massive groups, although they may never have been within the virial radius of the main cluster.

An important feature of this model is that many cluster galaxies at $z = 0.3$ have substantial SFRs. In particular, near R_{200}, $\sim 20\%$ of cluster galaxies have SFRs in excess of $1 M_{\odot}\mathrm{yr}^{-1}$, and this declines to about 10% at $R = 0.5 R_{200}$; fractions which are consistent with the CNOC1 data. These large SFRs are not the result of cluster-induced starbursts, but correspond to recently accreted field galaxies in which star formation has not yet been completely quenched. In a recent study, Balogh & Morris (**?**) have measured Hα equivalent widths for galaxies in Abell 2390, and they failed to find a substantial population with large Hα fluxes that were undetected in [OII]. Thus, there does not appear to be a population of dust-obscured starburst galaxies in this cluster which were missed in the CNOC1 survey. Our modeling indicates that cluster-induced starbursts are not necessary to generate the levels of star formation seen in these clusters.

We conclude from this comparison that a model based on the simple assumption that the SFR of a galaxy decreases on gas consumption timescales is able to reproduce the data extremely well, lending support to the underlying hypothesis that continuous accretion of external gas is responsible for maintaining the SFRs of normal spirals over a Hubble time.

5.2. *Evolving field SFR model*

There are two weaknesses in the model explored in the previous sections. One is the assumption that the SFRs of field galaxies, which are used to assign "initial" SFRs to cluster galaxies at accretion time (see eq. 3), do not evolve with time. Given the mounting evidence that the average SFR per unit volume evolves strongly with lookback time (**?**; **?**) it is necessary to explore the consequences of relaxing the non-evolving SFR assumption on our results. The second is the luminosity evolution of cluster galaxies, which must also be modeled in order to account for galaxies that may fade beyond the observational magnitude limit when their SFR declines.

A proper treatment of these effects, which must take into account the merger and star formation history of galaxies, is of great interest, but well beyond the scope of this study. In order to at least explore the effects that this more complete treatment will have, we use simple $\tau-$models to model the SFR evolution of field galaxies in our sample, i.e., by assuming that,

$$\dot{M}_*(t) = \dot{M}_*(t_0)\, \mathrm{e}^{-(t-t_0)/\tau}, \tag{4}$$

where $\dot{M}_*(t_0)$ corresponds to the SFR of galaxies in the field at $t = t_0 \approx 11$ Gyr, the age of the universe at $z \sim 0.3$. Once τ is determined for each galaxy it is possible to construct, at arbitrary times, an "evolving" field SFR distribution which matches the observations at $z \sim 0.3$. For a given IMF, and constant reddening, τ is uniquely determined by the observed $(g-r)_\circ$ color [6] of the galaxy, as shown in Figure 2. We have used the PEGASE (**?**) spectrophotometric models with a Salpeter IMF (with lower and upper limit given by $0.1 < M/M_\odot < 120$) to determine τ for each galaxy in our field sample. The bluest galaxies ($(g-r)_\circ < 0.04$) have $\tau < 0$, corresponding to a SFR that increases with time, while moderately blue galaxies ($(g-r)_\circ \approx 0$) have τ approaching (positive or negative) infinity, corresponding to a constant SFR. The reddest field galaxies, those with $\tau < 300$ Myr, are assumed to have formed in a single burst at high redshift, and are modeled as such in the cluster. The net result is a rather extreme model where the global star formation rate in the field population increases steadily out to $z \approx 10$. We explore below as well the consequences of restricting this increase at large z, and conclude that our results are quite insensitive to the precise nature of the redshift evolution in the field.

The normalization constant of eq. 4, $\dot{M}_*(t_0)$, may in principle be determined by the *observed* field galaxy SFR at t_0, but we found that, because of the large uncertainties in individual SFR determinations, this procedure leads to large discrepancies in the total luminosity of galaxies in the sample once the SFRs are integrated over time. Because total luminosities are considerably better determined than SFRs in our dataset, and are less sensitive to burst–like events that eq. 4 cannot reproduce, we compute $\dot{M}_*(t_0)$ for each field galaxy by requiring the model to reproduce its observed total Gunn-r luminosity at $z = 0.3$. This choice implies that, on a galaxy by galaxy basis, the model $z = 0.3$ SFRs no longer correspond to those derived from the $W_\circ$(OII) measurements. The observed and model field SFR distributions are compared in the bottom right panel of Figure 3; where the coefficient in eq. 1 (3.4×10^{-12}) has been chosen so that both distributions have identical averages. Although the difference is statistically significant, the two distributions are qualitatively fairly similar, indicating that, on average, the simple τ-model provides a reasonable description of the $z = 0.3$ field. This consistency allows us to compare model and observed SFRs, even though the former is based on galaxy color, while the latter is determined from nebular emission.

A further advantage of modeling the SFR history of the field population is that it allows us to model the color evo-

[6] This color is available for all galaxies in the CNOC1 dataset. We have made a small adjustment to the zero point of the observed $(g-r)_\circ$ colors, reducing them by 0.05 so that the reddest observed galaxies have the colors predicted by a model in which all stars formed at $t = 0$ in an instantaneous burst.

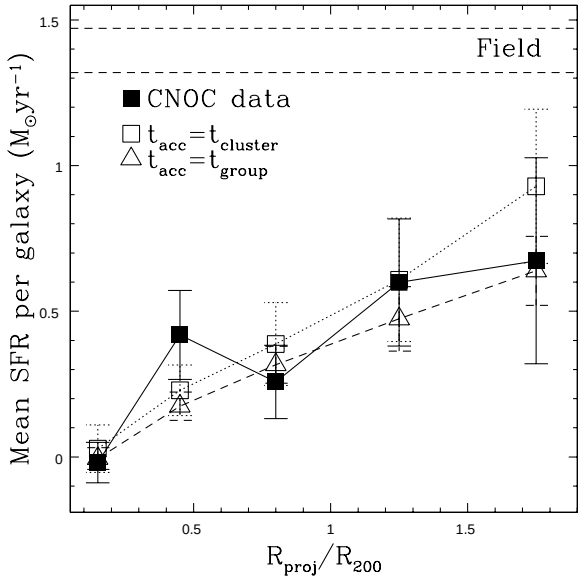

FIG. 1.— The mean SFR per galaxy as a function of projected radius for galaxies in the CNOC1 cluster sample (solid squares) compared with the model predictions under the assumption that $t_{\rm acc} = t_{\rm cluster}$ (open squares) and that $t_{\rm acc} = t_{\rm group}$ (open triangles). The horizontal dashed lines correspond to the field SFR, bracketed by its 1-σ dispersion. The SFR gradient in the CNOC1 clusters is accurately reproduced by our simple accretion models. Error bars are all 1σ.

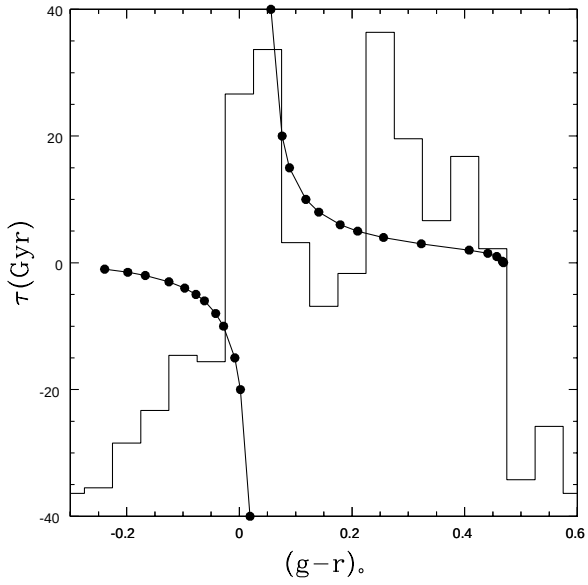

FIG. 2.— The histogram shows the distribution of $(g-r)_\circ$ colors for the field galaxy sample, in arbitrary units. The solid symbols correspond to model colors at $z = 0.3$ (an age of 11 Gyr) for galaxies with star formation history given by eqn. 4 and parameter τ as shown on the ordinate axis. The solid line through these points is the linear interpolation used to assign τ to each galaxy, based on its observed $(g-r)_\circ$.

lution of cluster galaxies. Color ($(g-r)_\circ$) distributions of model galaxies (which include the addition of a Gaussian random number to account for the 0.02 magnitude error typical of the CNOC1 data) are compared with the observational data in the left panels of Figure 3. The model shown adopts $t_{\rm acc} = t_{\rm group}$, and excludes galaxies fainter than $M_r = -19.6$ at $z = 0.3$. This model is very successful at producing a cluster core dominated by red galaxies from an initial field galaxy sample that has a much broader and bluer color distribution. In the outskirts of the cluster, both the observed and model color distributions show a significant increase in the population of blue galaxies. The qualitative agreement between model and observed SFR and color distributions throughout the cluster is quite remarkable for such a simple prescription.

The right panels of Figure 3 compare the observed SFR distributions with this same model. In agreement with observations, model distributions show a strong reduction in the fraction of galaxies forming stars at rates higher than about $\sim 1 M_\odot$ yr^{-1} near the cluster center. The agreement between model and observations is quite good, although model galaxies form stars at slightly higher rates in both bins.

The differences between model and observed mean cluster SFRs are clearly apparent in Figure 4, which shows the clustercentric gradient predicted by three variants of the evolving field-SFR model. The open circles correspond to the fiducial model as described above, and are generally larger than the observed cluster mean. The open triangles show how this result changes if we neglect galaxy fading; i.e., when we include all cluster galaxies in the average. This recovers the good match to the data, and shows that it is primarily the luminosity fading of galaxies that affects our result, and not the nature of the redshift evolution itself. To demonstrate this explicitly, we present a model (open squares) in which the field galaxy SFRs are evolved as in the fiducial model but are held constant for $z > 1.5$. The results obtained with this model do not differ significantly from those of the fiducial model, lending support to our conclusion that our results depend only mildly on the SFR redshift evolution.

We wish to stress that the purpose of the above exercise is to assess the sensitivity of our modeling to various assumptions about the redshift dependence of the SFR of the field galaxy population rather than to build a realistic model of field galaxy evolution. We conclude that the luminosity evolution of the field galaxies has a small, but non-negligible effect on our results. Although it appears that qualitatively our conclusions are safe, it is clear that definitive answers will have to wait for a more realistic modeling of the field galaxy star formation evolution, such as the one implemented in semianalytic models of galaxy formation (e.g. **?**, Diaferio et al. in preparation).

6. DISCUSSION

We present models of the clustercentric dependence of star formation and colors of galaxies in rich clusters, under the following assumptions: (i) the cluster galaxy population is built by the ongoing accretion of field galaxies, (ii) SFRs in field galaxies are sustained by regular accretion of gas from their surroundings, and (iii) reservoirs of fresh star formation fuel are lost as galaxies plunge into the cluster potential.

Within this context, our model provides support for a gradual decline (over a timescale of a few Gyrs) in the star formation rates of cluster galaxies after accretion. Actually, results similar to those presented in the previous section may be obtained if the SFR in *all* cluster galaxies is assumed to decay exponentially after accretion with fixed timescales $1 \lesssim t_e \lesssim 3$ Gyrs. Decline timescales longer than ~ 3 Gyr lead to unacceptably large star formation rates in model clusters at $z \sim 0.3$. On the other hand, sharp truncation of star formation ($t_e \lesssim 1$ Gyr) would result in too little star formation within clusters and, furthermore, would lead to an abundant population of galaxies with strong Balmer lines but no nebular emission lines (K+A galaxies), and these appear to be rare in the very luminous X-ray clusters we study here (**?**). Larger fractions of K+A galaxies have been reported in other cluster datasets, in particular by the MORPHS collaboration (**?**; **?**), but it is still unclear whether this apparent disagreement is a result of the procedure used to select the spectroscopic sample, the effects of dust obscuration, or perhaps a genuine effect of the dependence of SFRs on other cluster properties such as X-ray luminosity or temperature (**?**). Further analysis is required in order to assess whether the simple model we propose here is applicable to clusters other than the relatively massive, X-ray luminous systems targeted by the CNOC1 survey.

With this caveat, the success of our model strongly suggests that (i) gradients in galaxy properties arise from gradients in accretion times and (ii) that the cessation of star formation need not take place abruptly to explain the observed SFRs of cluster galaxies. On the other hand, our understanding of the star formation history of cluster galaxies is bound to remain incomplete until the physical mechanism responsible for the decline of star formation in cluster galaxies is fully elucidated. The loss of external gas reservoirs advocated here is attractive, but conclusive observational evidence that such reservoirs exist in isolated field galaxies has been slow to emerge (**?**, but see **?**). Other processes that may reduce star formation rates, such as tides, harassment, and ram pressure tripping, operate on similar timescales once a galaxy has been accreted into the cluster and it is therefore unlikely that analysis of the kind we present here will be able to distinguish clearly amongst them.

Another major question that our models do not address is the origin of gradients in galaxy morphology that parallel the color and star formation gradients we focus on (e.g., **?**; **?**; **?**). The over-representation of ellipticals near the center of X-ray luminous clusters may reflect higher merger rates between nearly equal mass systems in systems that collapse early to form cluster cores, but this is an issue that remains unexplored in our model. The construction of large spectroscopical datasets that probe the dependence of galaxy SFRs, colors and morphologies on cluster properties such as concentration, richness, velocity dispersion and X-ray properties, coupled with numerical and/or semianalytical models that treat self-consistently the accretion history and dynamics (and hydrodynamics) of galaxy and cluster formation, are probably the most promising way to make substantial progress in the subject.

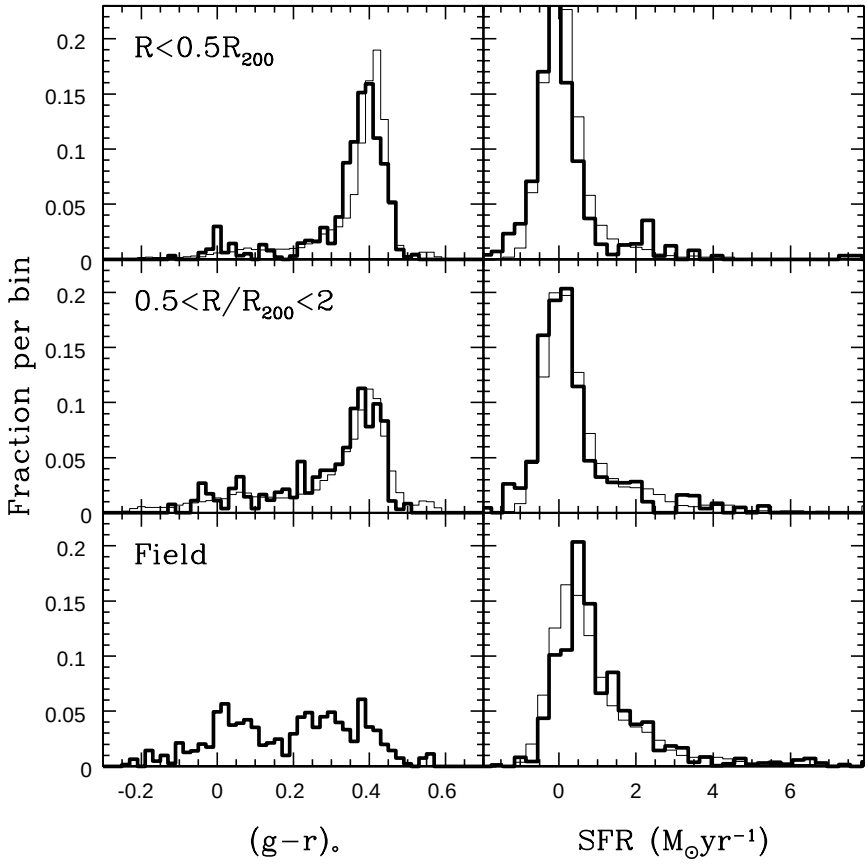

FIG. 3.— *Left panels:* $(g-r)_\circ$ distributions in the observed CNOC1 sample (*heavy solid lines*) and our evolving field-SFR model (*thin solid lines*). The samples are divided into a field sample and two cluster samples (inner and outer regions), as labeled in each panel. By construction, the model color distribution matches the field observations exactly. *Right panels:* SFR distributions for the same samples shown in the left panels. The model provides a good match to the color and SFR distributions of the observed cluster population, although it slightly overestimates the mean cluster SFR.

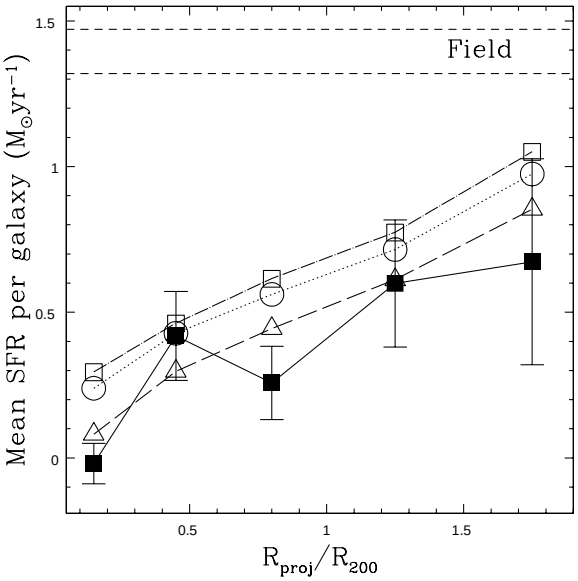

FIG. 4.— Same as Figure 1 but for three evolving field SFR models. In the fiducial model (open circles), the SFRs in field galaxies evolve as dictated by simple τ models normalized to match the colors of field galaxies at $z \sim 0.3$, and galaxies that fade below the luminosity limit are excluded (see §5.2). Accretion times are defined as $t_{\rm acc} = t_{\rm group}$. The open squares show the result of modifying the evolution such that each galaxy's SFR remains constant at $z > 1.5$. Neglecting the effects of galaxy fading in the fiducial model results in the open triangles. The data are shown by the filled squares, connected by the solid line.

7. CONCLUSIONS

We present a simple model to account for the systematic differences in the star formation properties of galaxies in CNOC1 clusters and the field. The model assumes that the cluster is built through the accretion of field galaxies whose star formation rates gradually decline after entering the cluster as a result of the removal, through tides or ram pressure, of the gaseous envelopes needed to supply normal spirals with the fuel needed to sustain their present star formation rates over a Hubble time. Once calibrated to reproduce observations of nearby spirals the model has no free parameters.

Using cluster mass accretion rates determined from N–body simulations of cluster formation in a ΛCDM universe, our model is able to reproduce qualitative and quantitative differences in the mean star formation rates and colors between clusters and the field. The model demonstrates that the origin of radial gradients in these properties is the natural consequence of the strong correlation between radius and accretion times which results from the hierarchical assembly of the cluster. Interestingly, the model also explains why star formation in the outskirts of clusters is found to be almost a factor of two below the field average as far out as twice the virial radius of the cluster. This is a result of cluster members being pushed onto highly eccentric, loosely bound orbits during major merger events. Our results are robust to evolution in the star formation properties of field galaxies, but somewhat more sensitive to the manner in which fading of cluster galaxies is modeled. Realistic modeling of the field population star formation histories is required to fully understand the consequences of this fading.

We conclude that the stripping of extended gaseous reservoirs by the cluster environment and the gradual decline that follows gas consumption is likely to be the main mechanism that differentiates the star formation properties of cluster and field galaxies.

We have made extensive use of the CNOC1 dataset of intermediate–redshift clusters. We are grateful to all the consortium members and to the CFHT staff for their contributions to this project. We thank the referee for a careful reading of the manuscript, and for useful suggestions which improved this paper. In Victoria, MLB was supported by a Natural Sciences and Engineering Research Council of Canada (NSERC) research grant to C. J. Pritchet and by an NSERC postgraduate scholarship. In Durham, MLB is supported by a PPARC rolling grant for extragalactic astronomy and cosmology.